Supporting information

Myo-inositol Supported heterometallic $Dy_{24}M_2$ (M = Ni, Mn) Cages

Da-Peng Liu, Jun-Bo Peng, Xin-Ping Lin, Que Huang, Xiang-Jian Kong,* La-Sheng Long,* Rong-Bin Huang, and Lan-Sun Zheng

State Key Laboratory of Physical Chemistry of Solid Surface and Department of Chemistry, College of Chemistry and Chemical Engineering, Xiamen University, Xiamen, 361005, China.

General Considerations. Caution! Perchlorates are potentially explosive. Only a small amount should used and handled with great care. All reagents were of commercial origin and were used as received. The C, H, and N microanalyses were carried out with a CE instruments EA 1110 elemental analyser. The infrared spectrum was recorded on a Nicolet AVATAR FT-IR360 Spectrophotometer with pressed KBr pellets. TGA curve was prepared on a SDT Q600 Thermal Analyzer. Magnetic susceptibility was measured by a Quantum Design MPMS superconducting quantum interference device (SQUID).

Preparation of aqueous solutions of $Dy(ClO_4)_3$ (1.0 mol L^{-1}). Dysprosium oxide (0.125 mol, 46.625 g) was dissolved by slowly adding perchloric acid aqueous solution (70.0% - 72.0%, 60.0 ml) at about 70 ^oC. Aqueous solution of $Dy(ClO_4)_3$ (1.0 mol L^{-1}) was obtained by diluting the concentrated solution to 250.00 ml with deionized water.

Synthesis of $[Dy_{24}Ni_2(OH)_8(C_2H_3O_2)_{12}(C_6H_{10}O_6)_6(C_6H_9O_6)_6(H_2O)_{51}]\cdot[Dy(H_2O)_9]\cdot(ClO_4)_{29}\cdot(H_2O)_{80}\cdot(C_2H_5OH)_4$ (1). $Ni(CH_3COO)_2\cdot 6H_2O$ (249 mg, 1.0 mmol), $Dy(ClO_4)_3$ (4 ml, 4.0 mmol) and myo-inositol (18 mg, 1.0 mmol) was added to a mixture of 10 mL anhydrous ethanol. The resulting solution was heated to about 70 ^oC and a freshly prepared NaOH solution (aq. 1.0 mol L-1) was added dropwise to adjust the pH of the solution to 6 while stirring. Then the solution was refluxed for 2 hours and then filtered. Evaporation of the filtrate under ambient conditions afforded 170 mg light green block crystals in two weeks (yield 16 % based on myo-inositol).

Anal. calcd. for $C_{104}H_{458}Dy_{25}Ni_2O_{364}Cl_{29}$ (FW = 12805.97): C, 9.80 H, 3.62; Found: C, 9.99; H, 3.51. IR (KBr, cm^{-1}): 3351 cm^{-1}, 1626 cm^{-1}, 1545 cm^{-1}, 1456 cm^{-1}, 1089 cm^{-1}, 902 cm^{-1}, 627 cm^{-1}.

Synthesis of $[Dy_{24}Mn_2(OH)_8(C_2H_3O_2)_{12}(C_6H_{10}O_6)_6(C_6H_9O_6)_6(H_2O)_{51}]\bullet[Dy(H_2O)_9]\bullet(ClO_4)_{29}\bullet(H_2O)_{80}\bullet(C_2H_5OH)_4$ (2). Compound **2** was prepared by the similar way as described for compound **1**, excepting using $Mn(CH_3COO)_2$ (245 mg, 1.0 mmol) to replace the $Ni(CH_3COO)_2{\cdot}6H_2O$. Evaporation of the filtrate under ambient conditions afforded 180 mg light yellow block crystals in two weeks (yield 17 % based on myo-inositol). Anal. calcd. for $C_{104}H_{458}Dy_{25}Mn_2O_{364}Cl_{29}$ (FW = 12799.98): C, 9.81; H, 3.62; Found: C, 9.88; H, 3.55. IR (KBr, cm^{-1}): 3351 cm^{-1}, 1626 cm^{-1}, 1545 cm^{-1}, 1456 cm^{-1}, 1384 cm^{-1}, 1088 cm^{-1}, 902 cm^{-1}, 627 cm^{-1}.

Single crystal X–ray structure determination: Data of compounds **1** and **2** were collected on an Oxford Gemini S Ultra CCD area detector with monochromatic Mo Kα radiation (λ = 0.71073 Å). Absorption corrections were applied by using the multiscan program CrysAlis Red. The structures were solved by direct methods, and non-hydrogen atoms were refined anisotropically,[1] except for C4 C6 C13 C14 O3w C5 O21 O22 C15 C2 C16 Cl2 and O23 for compound 1 and C1 C2 C3 C4 C5 C6 C7 C8 C9 C10 C11 C12 C13 C15 O18 and O11w for compound 2 were refined isotropically due to disorder. SQUEEZE removed 4 disordered ethanol molecules, 80 disordered water molecules and 24 ClO_4^- per formula unit for **1** and **2**. This valueis calculated based upon elemental analysis data and TGA data. The hydrogen atoms of the organic ligand were generated geometrically (C–H, 0.96 A). Crystal data as well as details of data collection and refinement for the complexes are summarized in Table 1. CCDC contains the supplementary crystallographic data for this paper with a deposition number of nos. 983777 for **1** and 9837778 for **2,** respectively. The crystallographic data can be obtained free of charge from The Cambridge Crystallographic Data Centre via http://www.ccdc.cam.ac.uk/data_request/cif.

1 SHELXTL 6.10, Bruker Analytical Instrumentation, Madison, WI, 2000

Table S1 Crystal data and details of data collection and refinement for **1–2**

COMPLEX	***1***	**2**
Formula	$C_{104}H_{458}Dy_{25}Ni_2O_{364}Cl_{29}$	$C_{104}H_{458}Dy_{25}Mn_2O_{364}Cl_{29}$
*M*r	12805.97	12799.98
Crystal system	Hexagonal	Hexagonal
Space group	P6(3)/m	P6(3)/m
a/Å	25.5089(9)	25.5250(11)
b/Å	25.5089(9)	25.5250(11)
c/Å	34.3318(17)	34.3906(14)
V/Å^3	19346.9(14)	19404.5(14)
Z	2	2
*D*c/g cm^{-3}	2.187	2.180
μ/mm^{-1}	5.191	5.143
Data/parameters	11507 / 489	11519 / 489
θ/^{o}	2.71-25.00	2.71- 25.00
Observed reflections	4113	3865
$R_1[I > 2\sigma(I)]$[a]	0.0893	0.0860
wR_2(All data)[b]	0.2274	0.2165

[a] $R_1 = \sum | |Fo| - |Fc| | / \sum |Fo|$ [b] $wR_2 = \{\sum [w (Fo^2 - Fc^2)^2] / \sum [w(Fo^2)^2]\}^{1/2}$

Table S2 Selected bonds and angles for **1.**

Ni(1)-O(10)	2.062(7)	Ni(1)-O(14W)	2.127(7)
Dy(1)-O(9W)	2.466(7)	Dy(1)-O(11)	2.250(8)
Dy(1)-O(14)	2.394(4)	Dy(1)-O(13)	2.418(7)
Dy(1)-O(16)	2.452(6)	Dy(1)-O(10)	2.455(6)
Dy(2)-O(18)	2.332(10)	Dy(2)-O(13)	2.346(6)
Dy(2)-O(7W)	2.398(10)	Dy(2)-O(5W)	2.467(9)
Dy(2)-O(4)	2.508(9)	Dy(2)-O(8)#2	2.541(12)
Dy(3)-O(11)	2.289(8)	Dy(3)-O(17)	2.315(9)
Dy(3)-O(5)	2.316(7)	Dy(3)-O(15)	2.359(8)
Dy(3)-O(13)	2.361(7)	Dy(3)-O(8W)	2.412(10)
Dy(3)-O(6)	2.429(9)	Dy(3)-O(12)	2.448(10)
Dy(4)-O(2)	2.251(8)	Dy(4)-O(1)	2.404(10)
Dy(5)-O(2)	2.320(8)	Dy(5)-O(3)	2.463(9)
Dy(1)#1-O(9)-Dy(2)#1	114.5(3)	Dy(1)#1-O(14)-Dy(1)	109.3(3)
Dy(1)-O(11)-Dy(3)	112.2(3)	Dy(2)-O(13)-Dy(1)	108.2(3)
Dy(4)-O(2)-Dy(5)	110.1(3)	Dy(1)#1-O(10)-Dy(1)	106.4(2)
Dy(2)-O(5)-Dy(3)	110.1(3)	Dy(2)-O(13)-Dy(3)	106.0(3)
Dy(1)#2-O(14)-Dy(1)#1	109.3(3)	Dy(3)-O(13)-Dy(1)	104.1(2)
Dy(1)#2-O(14)-Dy(1)	109.3(3)	Ni(1)-O(10)-Dy(1)#1	101.9(3)
Ni(1)-O(10)-Dy(1)	100.9(2)		

Table S3 Selected bonds and angles for **2.**

Dy(1)-O(11)#1	2.235(7)	Dy(1)-O(9)	2.334(7)
Dy(1)-O(14)	2.397(4)	Dy(1)-O(13)	2.405(8)
Dy(1)-O(18)	2.424(7)	Dy(1)-O(10)	2.446(7)
Dy(1)-O(9W)	2.491(7)	Dy(2)-O(5)	2.270(9)
Dy(2)-O(9)	2.271(8)	Dy(2)-O(13)	2.340(7)
Dy(2)-O(16)	2.374(10)	Dy(2)-O(5W)	2.464(9)
Dy(2)-O(4)	2.510(8)	Dy(2)-O(8)	2.513(12)
Dy(2)-O(7W)	2.527(8)	Dy(3)-O(5)	2.301(8)
Dy(3)-O(15)	2.332(9)	Dy(3)-O(13)	2.344(8)
Dy(3)-O(17)	2.401(8)	Dy(3)-O(8W)	2.484(10)
Dy(3)-O(6)	2.489(9)	Dy(4)-O(2)	2.248(9)
Dy(4)-O(3W)	2.34(2)	Dy(4)-O(4W)	2.353(18)
Dy(4)-O(1)	2.434(8)	Dy(4)-O(10W)	2.47(2)
Dy(5)-O(2)	2.260(9)	Dy(5)-O(1W)	2.37(2)
Dy(5)-O(2W)	2.38(2)	Dy(5)-O(3)	2.461(8)
Dy(5)-O(13W)	2.68(3)	Dy(6)-O(11W)	2.28(4)
Dy(6)-O(12W)	2.507(14)	Mn(1)-O(10)	2.189(6)
Mn(1)-O(14W)	2.217(7)		
Dy(2)-O(13)-Dy(3)	106.8(3)	Dy(2)-O(13)-Dy(1)	109.2(3)
Dy(3)-O(13)-Dy(1)	104.8(2)	Mn(1)-O(10)-Dy(1)	101.4(3)
Dy(2)-O(9)-Dy(1)	114.3(3)	Dy(2)-O(5)-Dy(3)	110.7(3)
Dy(4)-O(2)-Dy(5)	111.8(3)		

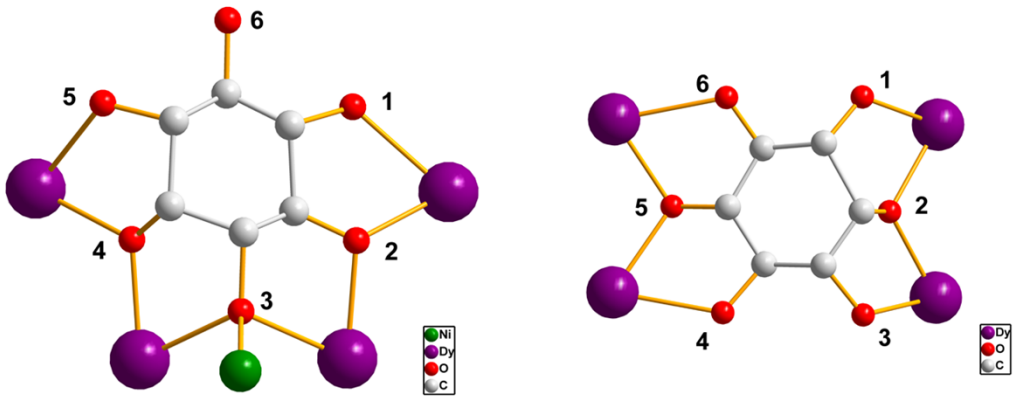

Figure S1. Two different coordination modes of myo-inositol ligand in compound **1**.

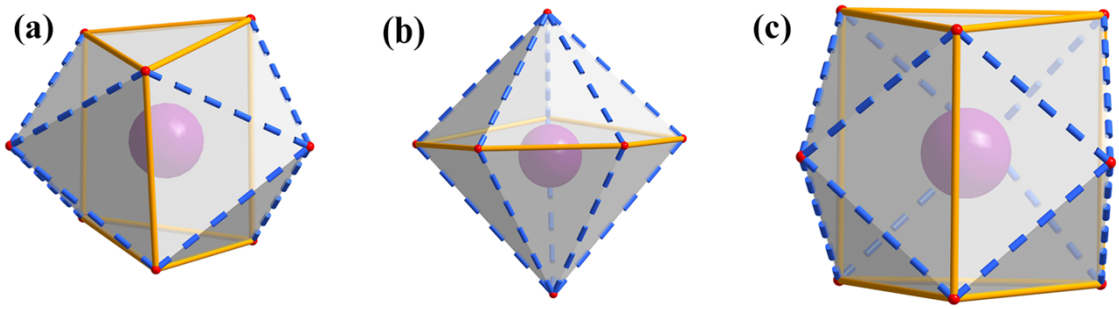

Figure S2. Three different coordinate geometries for Dy1, Dy2, Dy3, and Dy4 (a), Dy5 (b), and Dy6 (c).

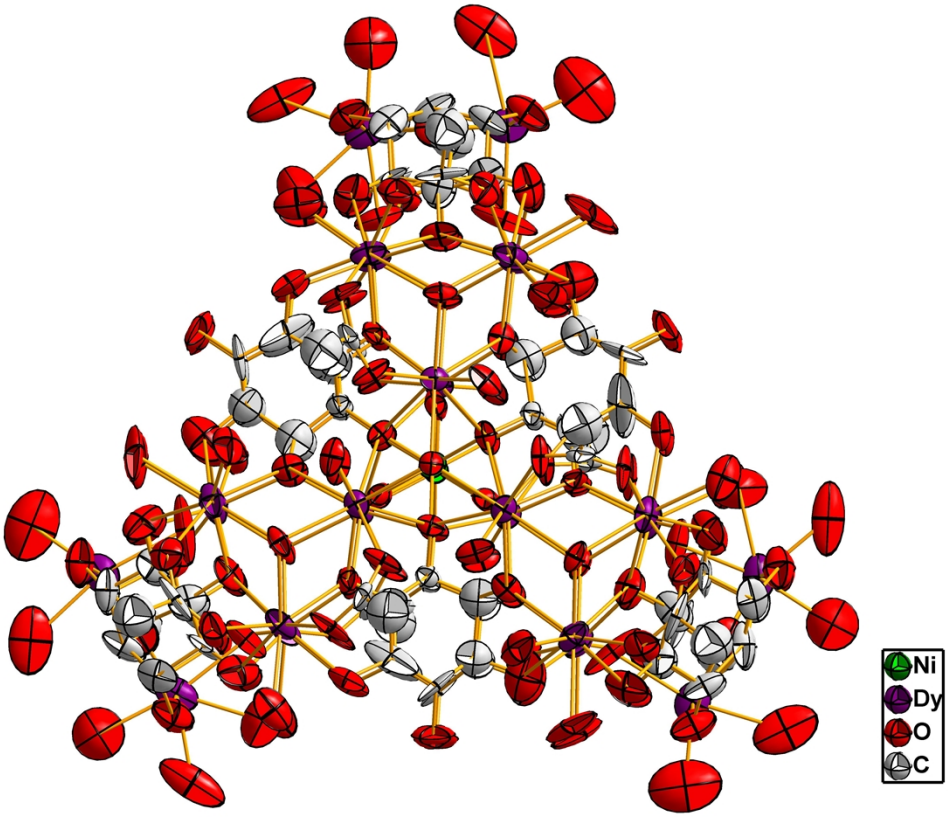

Figure S3 The ORTEP view of 1

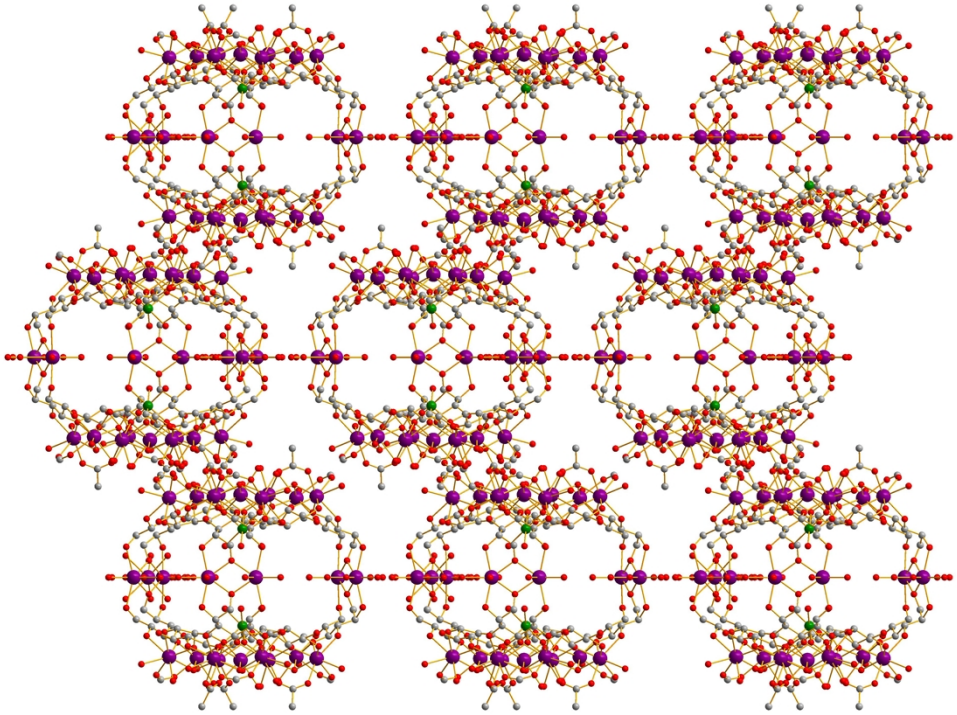

Figure S4. Ball and stick view of the packing for **1**.

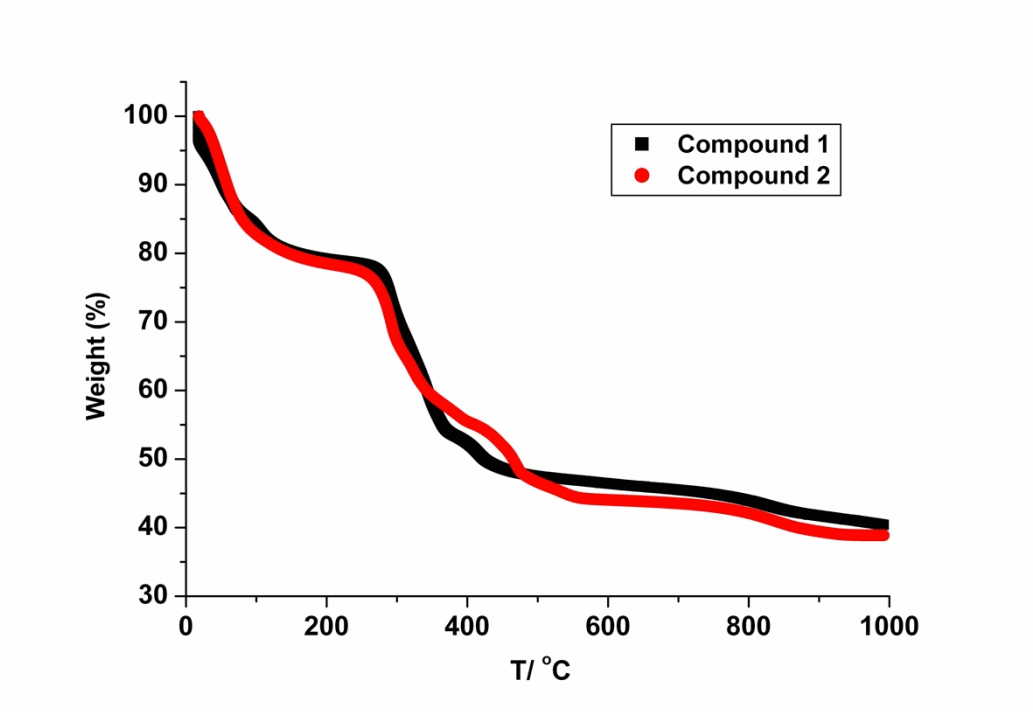

Figure S5. TG Curves for compounds **1**-**2**.

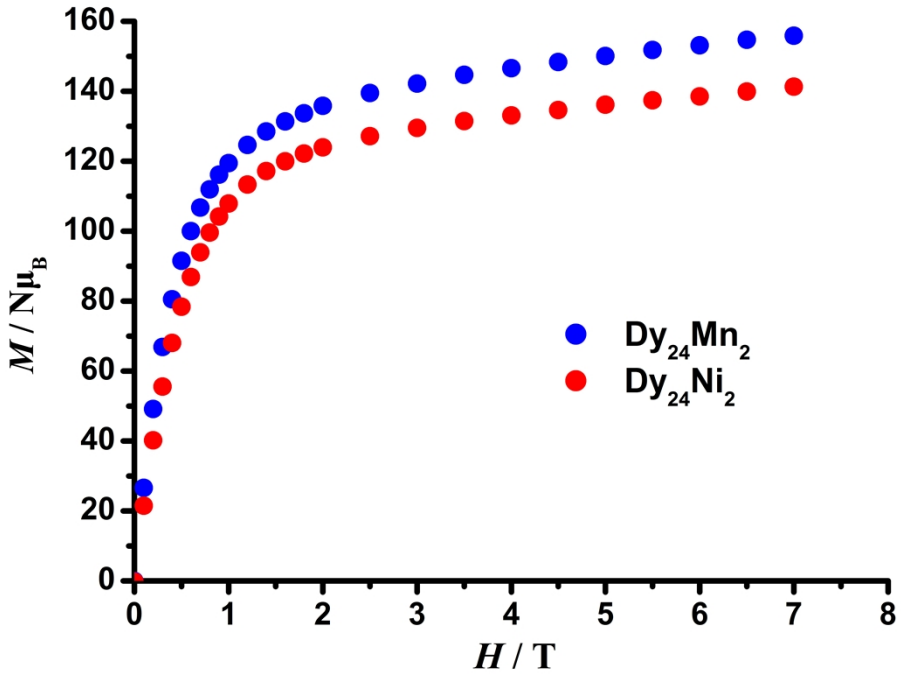

Figure S6. Magnetization versus *H*/*T* for **1** and **2** at 2.0 K and at indicated fields.

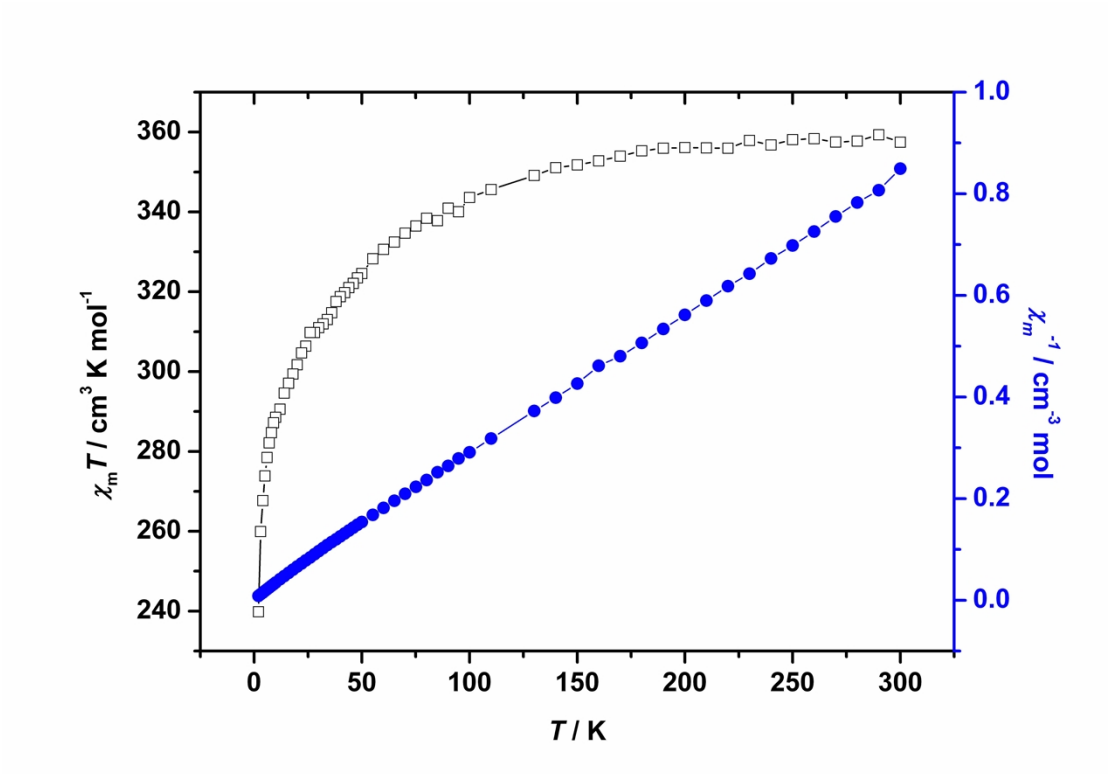

Figure S7. Plots of temperature dependence of $\chi_M T$ (□) and χ_M^{-1} (●) for **1** under 1000 Oe dc field between 2 and 300 K.

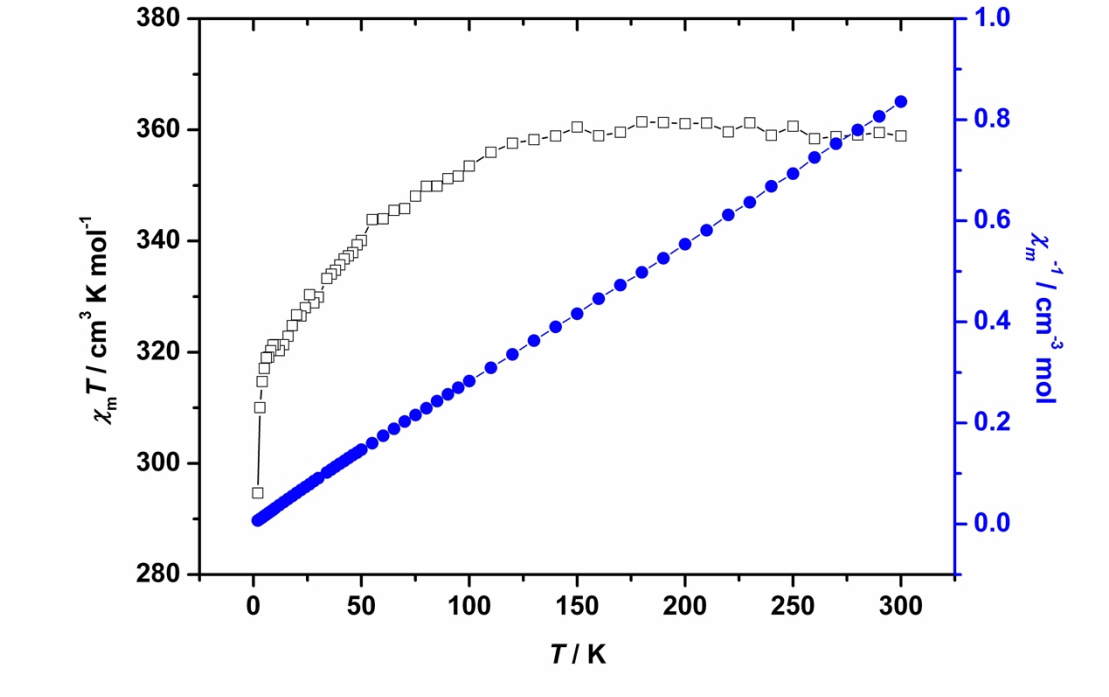

Figure S8. Plots of temperature dependence of $\chi_M T$ (□) and χ_M^{-1} (●) for **2** under 1000 Oe dc field between 2 and 300 K.

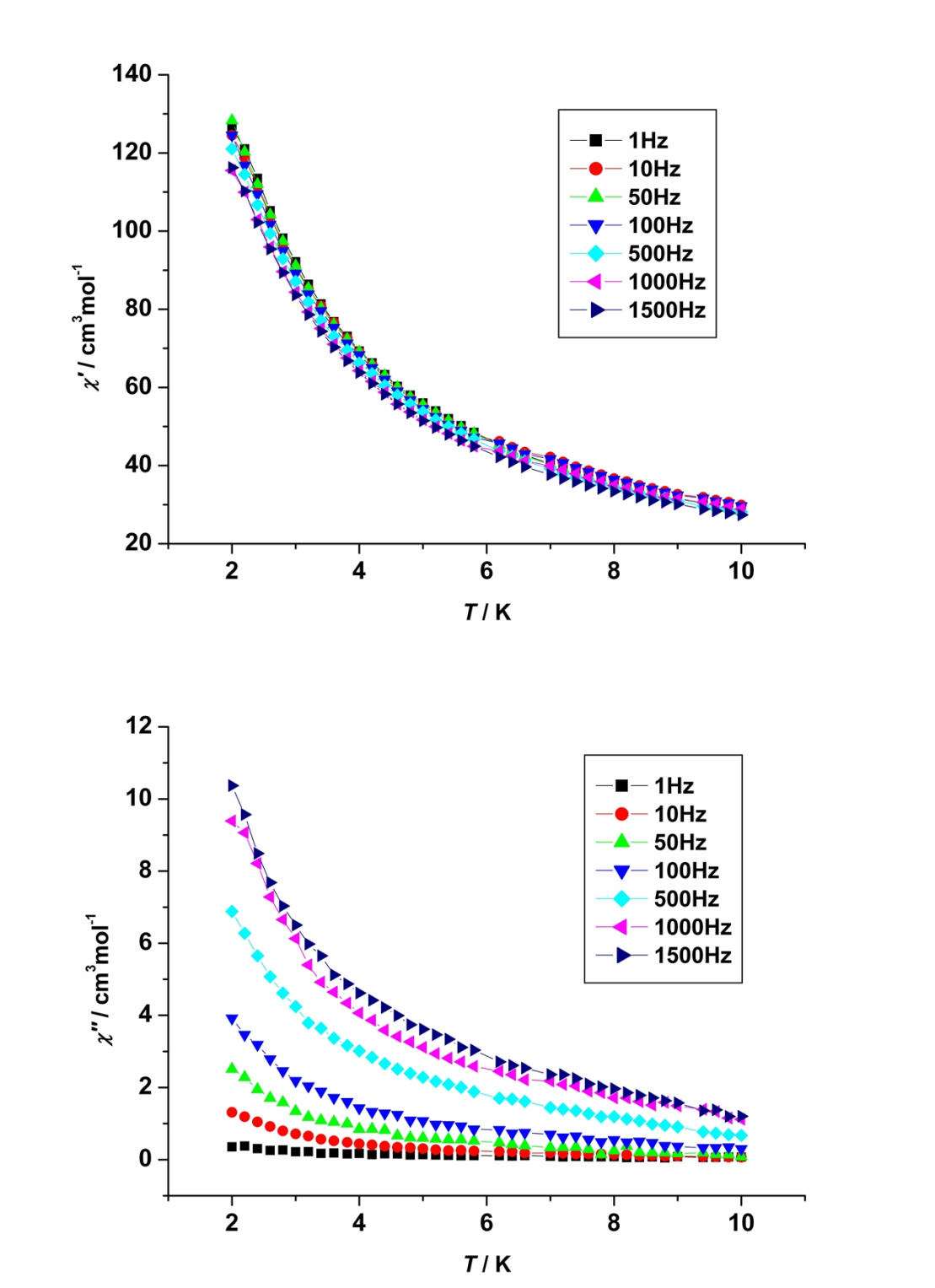

Figure S9. Temperature dependence of the in phase (a) and out-of-phase (b) ac susceptibilities at the indicated frequencies for **1**.

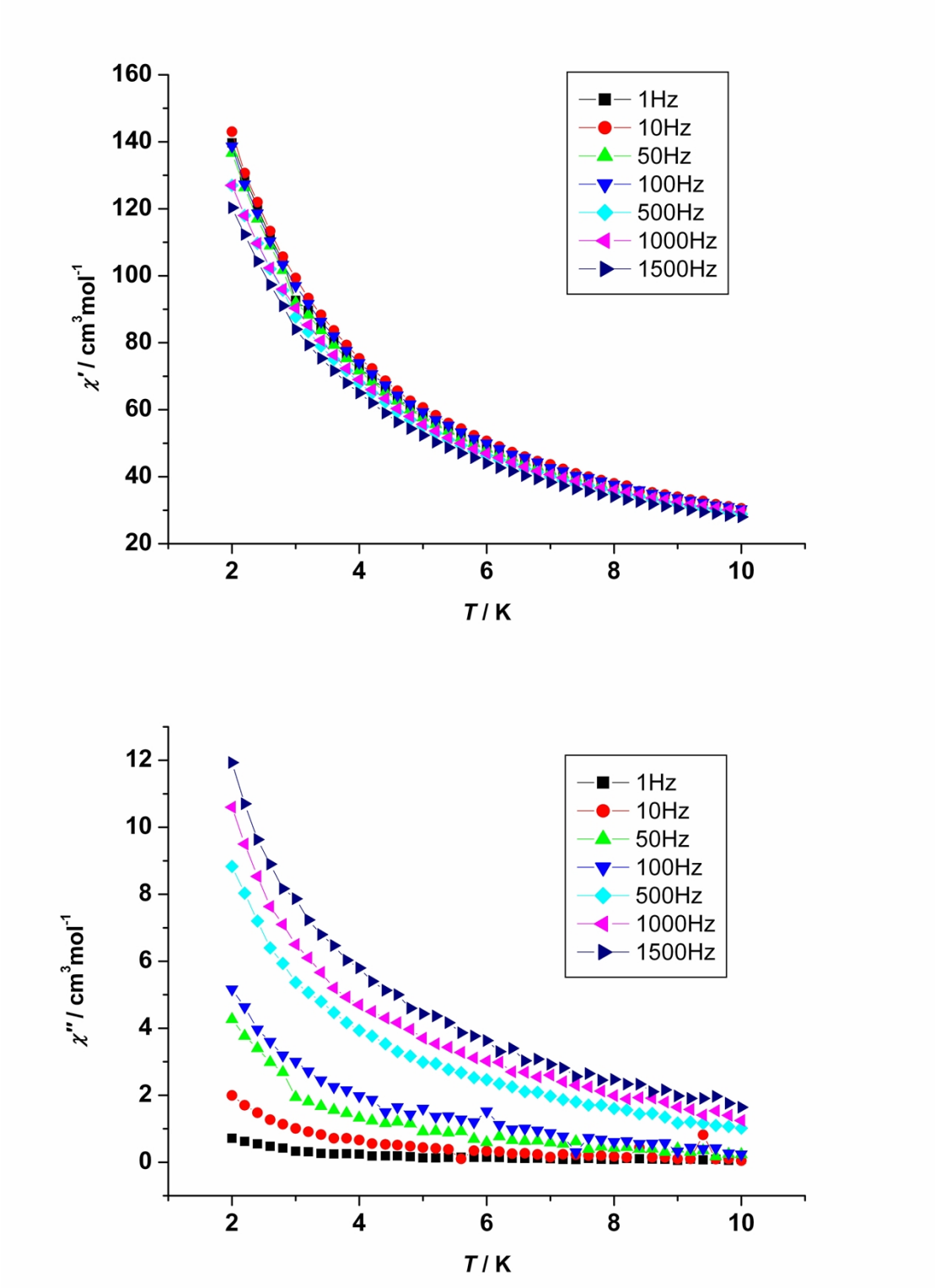

Figure S10. Temperature dependence of the in phase (a) and out-of-phase (b) ac susceptibilities at the indicated frequencies for **2**

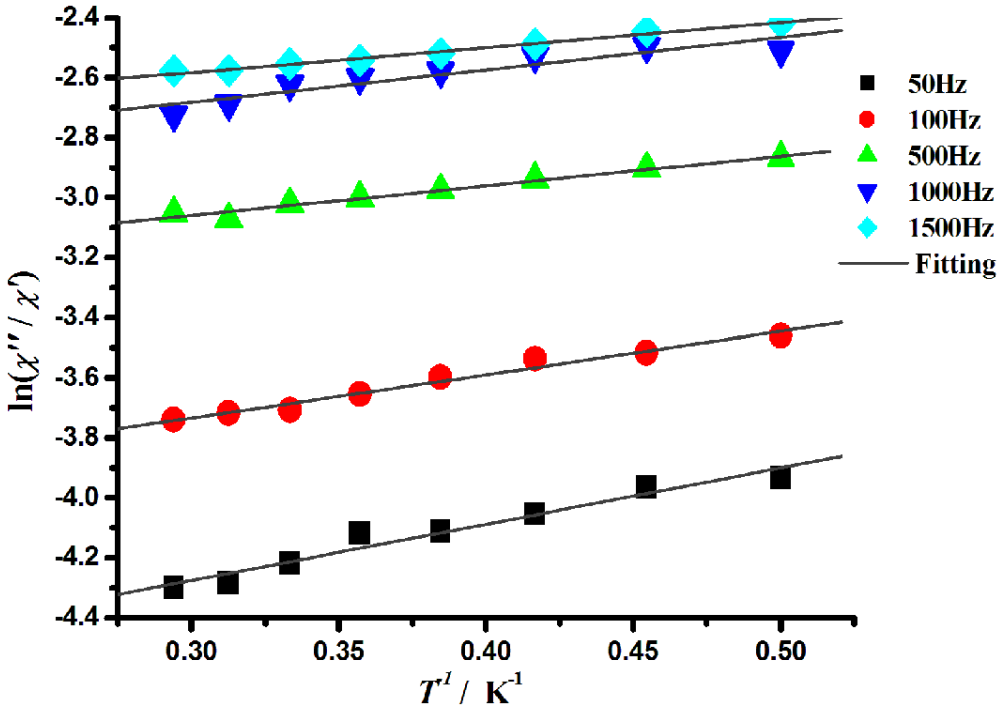

Figure S11. Plots of natural logarithm of χ″/χ′ vs 1/*T* for **1**. The solid line represents the fitting results over the range 2.0–3.2 K.

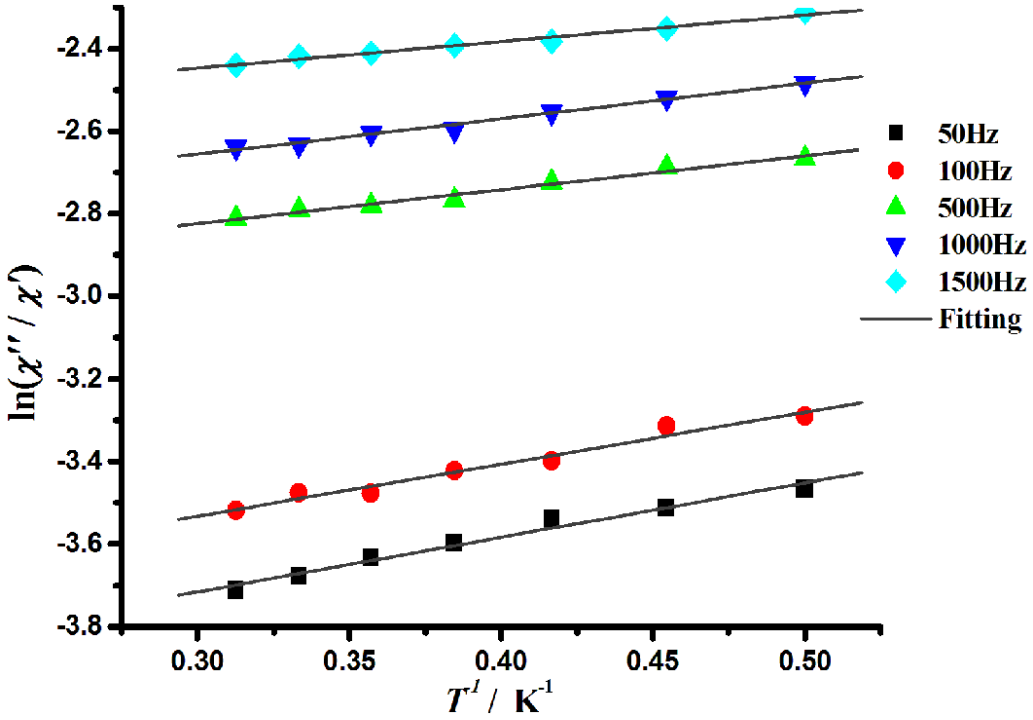

Figure S12. Plots of natural logarithm of χ″/χ′ vs 1/*T* for **2**. The solid line represents the fitting results over the range 2.0–3.2 K.